LASER INTERFEROMETER GRAVITATIONAL WAVE OBSERVATORY
- LIGO -
CALIFORNIA INSTITUTE OF TECHNOLOGY
MASSACHUSETTS INSTITUTE OF TECHNOLOGY

Technical Note	**LIGO-T2000647-v1**
Stress Analysis of Thermal SAMS Assembly	
Huy Tuong Cao	

This is an internal working
note of the LIGO project.

California Institute of Technology
LIGO Project, MS 18-34
Pasadena, CA 91125
Phone (626) 395-2129
Fax (626) 304-9834
E-mail: info@ligo.caltech.edu

Massachusetts Institute of Technology
LIGO Project, Room NW17-161
Cambridge, MA 02139
Phone (617) 253-4824
Fax (617) 253-7014
E-mail: info@ligo.mit.edu

LIGO Hanford Observatory
Route 10, Mile Marker 2
Richland, WA 99352
Phone (509) 372-8106
Fax (509) 372-8137
E-mail: info@ligo.caltech.edu

LIGO Livingston Observatory
19100 LIGO Lane
Livingston, LA 70754
Phone (225) 686-3100
Fax (225) 686-7189
E-mail: info@ligo.caltech.edu

WWW: http://www.ligo.caltech.edu/

Contents

1 Introduction 3

2 Finite element model 3

3 Stresses in Macor strut 4

4 Torque on the Macor strut - manifold connection 5

5 Fastener rotation 6

1 Introduction

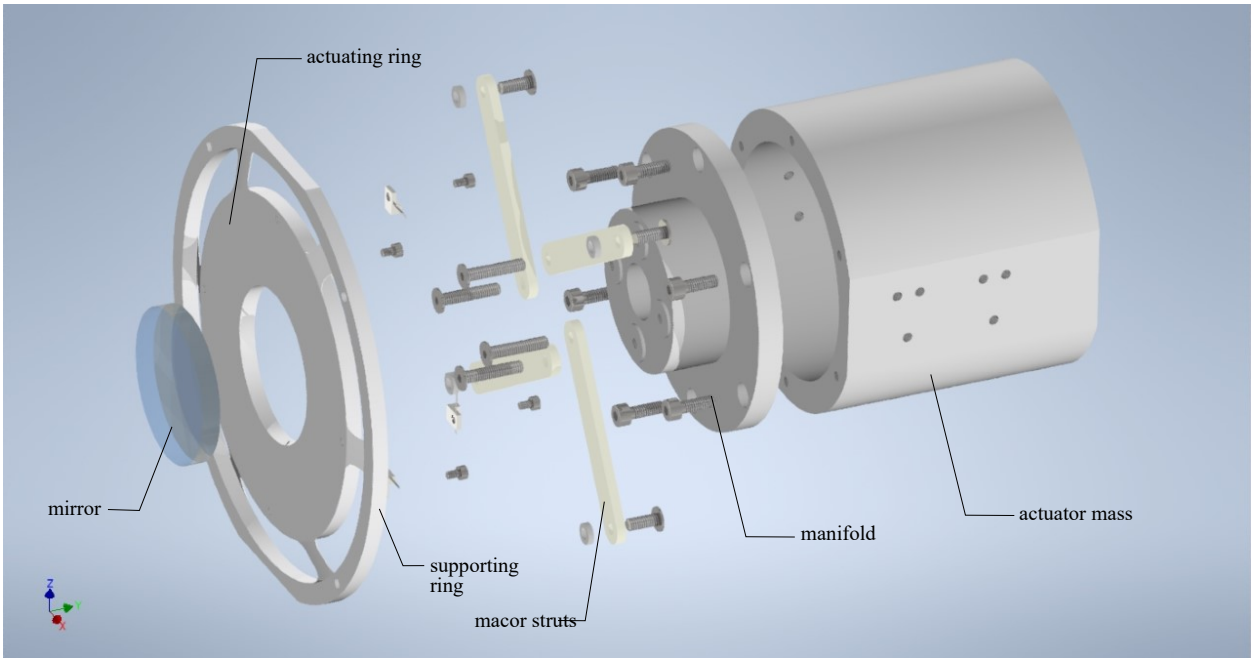

Figure 1: Exploded view of the thermal compression-fit mirror assembly, showing macor struts connecting the supporting ring to the manifold (Note that in the final design, the flexure connecting the actuating ring and the supporting ring does not have any cut-out.

The following document investigates the stress in mounting structure of the thermal SAMS mirror. The SAMS mirror consists of an actuating ring, a supported ring, connected by a conical flexure. The supporting ring is secured on a manifold by 4 Macor struts, as seen in Fig. 1. During actuation, thermal expansion of the thermal SAMS would induce stress in the macor strut. The goal of this document is to investigate whether the stress in the macor strut and the torque on the screw connecting struts to the manifold.

2 Finite element model

Fig. 2 shows the isotropic view and the rear view of the finite element model of CFM assembly. We only simulate a quadrant of structure to speed up simulation time. Symmetry boundary condition is applied on cut surfaces of that result in the quadrant. The actuator mass is also not included in this simulation since it doesn't affect the distribution of stress in the macor struts.

All contact is assumed to be "glued" contact since modeling contact between screw and thread is a complex problem and often does not present accurate result.

In this model, manifold is constrained to be a fixed domain, considering its significantly higher stiffness, compared to other domains. A temperature of 60°C which is the maximum operating temperature is applied to the actuating ring. All surfaces heat transfer boundary condition are set to radiative heat transfer to ambient. The ambient temperature is assumed

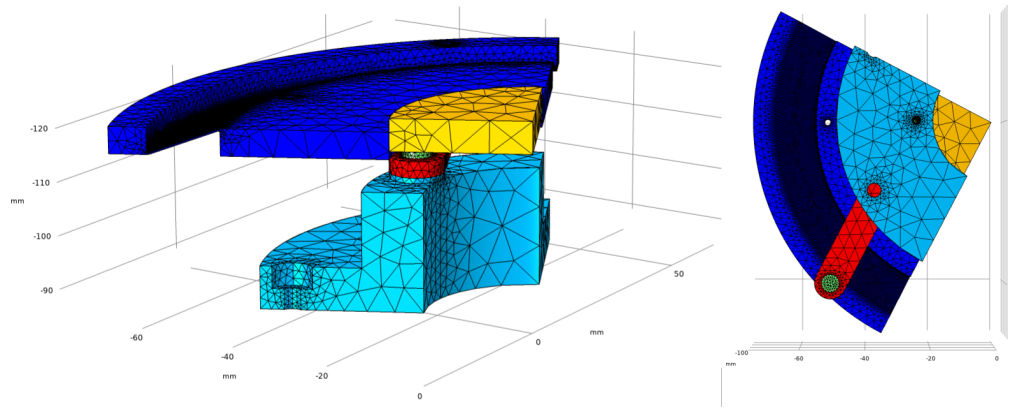

Figure 2: 3D finite element model of the CFM manifold-strut-actuator assembly

to be 298.15 K. The emissivities of fused silica, macor, and aluminium are set to 0.93, 0.9 and 0.3 respectively.

`Thermal Expansion` from COMSOL MULTIPHYSICS module is used to couple the change in temperature to `Solid Mechanics` module, which simulates the deformation of the structure. The reference strain temperature is the ambient temperature. Deformation simulated is relatively to that at ambient temperature, instead of the absolute deformation. This is acceptable since our main interest in the deformation and stress in the macor struts, which are assembled at ambient temperature.

3 Stresses in Macor strut

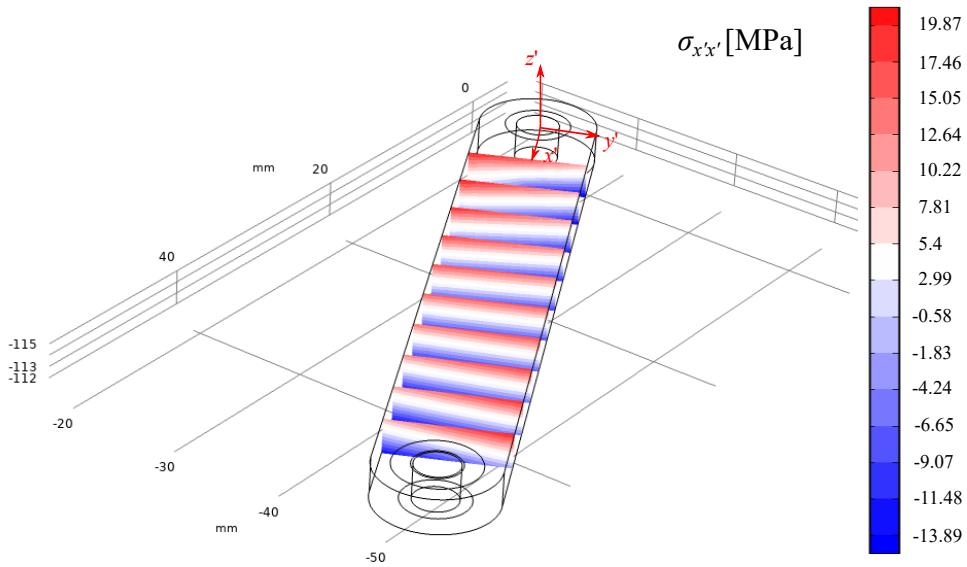

Figure 3: Tensile stress and compressive stress along x'-direction

The conical deformation of the supporting ring induces a downward force along the z'-direction (Fig. 3) on the macor struts, resulting in a moment $M_{y'}$, causing the strut to bend

downwards, about y'-axis. Radial thermal expansion of the ring structure also results in a transverse force bending the strut about the z'-axis. These bendings result in tensile an compressive stress distribution in $\sigma_{x'x'}$, as shown in Fig. 3. This shows that the maximum tensile stress in the strut is approximately 21 MPa. The modulus of rupture, (or flexural strength), which measures the tensile stress just before the material yields under bending test, is 94 MPa, according to Corning specification Corning SAS. Using this number, we have safety factor of 4.5.

The maximum compressive stress in $\sigma_{x'x'}$ is 14 MPa. The compressive strength of Macor is 345 MPa. The safety factor is thus 24.6.

4 Torque on the Macor strut - manifold connection

The torque induced by the radial expansion of the actuating ring on the macor-manifold joint can be estimated from the deflection $dy'_{\max}$ around the z' axis at the end of strut that is in contact with the supporting ring. From FEA results, the maximum deflection at this point is 34 μm. For a cantilever with a fixed end and a transverse force V applied on one end. The deflection dy' is related to the force V by:

$$|\delta y'|_{\max} = \frac{VL^3}{3EI} \tag{1}$$

where L is the length of the strut, which is 57.15 mm, E is the Young's modulus of Macor and I is the second moment of area, which in our case is given by $tw^3/12$. For $t = 3.05$ mm and $w = 9.9$ mm, I is $2.47\times10^{-10}\text{m}^4$. Rearranging for V, we found that V is is approximately 9 N. The torque acting on the screw is therefore $9[\text{N}]\times57.15\times10^{-3}[\text{m}] = 0.5$ N·m

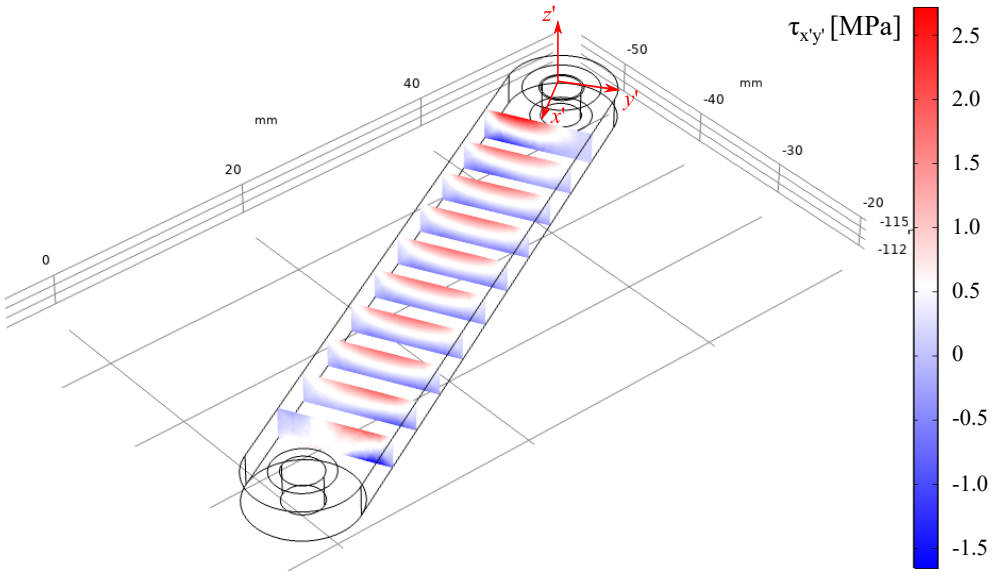

Figure 4: Shear stress $\tau_{x'y'}$ in the Macor strut caused by the CFM deformation

We can furtherverify this by analysing the shear stress within the strut. Fig, 4 shows the shear stress $\tau_{x'y'}$ in the Macor strut caused by the radial expansion of heating the CFM. This

shear stress distribution is a result of two mechanism: the y' transverse force bending about the z' axis and the pulling along x' axis. The second mechanism results in the linear variation in shear stress along the z' axis, across the strut cross section. The bending about the z' axis is the effect of interest which is related to the torque. This effects induces a quadratically varying shear stress along the y' axis. To investigate this effect only, we evaluate the shear stress at the neutral plane of the $z'y'$-cross-section , which is the mid-plane. The average shear stress is then related to the transverse force by:

$$V = \tau_{\text{ave}} A = \tau_{\text{ave}} t w \tag{2}$$

The average shear stress obtained from the FEA model is 0.41 MPa. The approximate transverse force V is therefore 8.4 N. The torque is thus also approximately 0.5 N·m. The recommended tightening torque for the 8-32 screw is 25.8 In lbs, which is approximately 3 Nm. This thus has a safety factor of 6, not including the fact it will need higher torque to overcome the initial static friction after tightening, likely to be 2-3 times higher than the tightening torque.

5 Fastener rotation

In order to determine the effect of strut rotation on the assembly the radial expansion (δr)of the actuation ring at the location of the fasteners was evaluated from the FEA model.

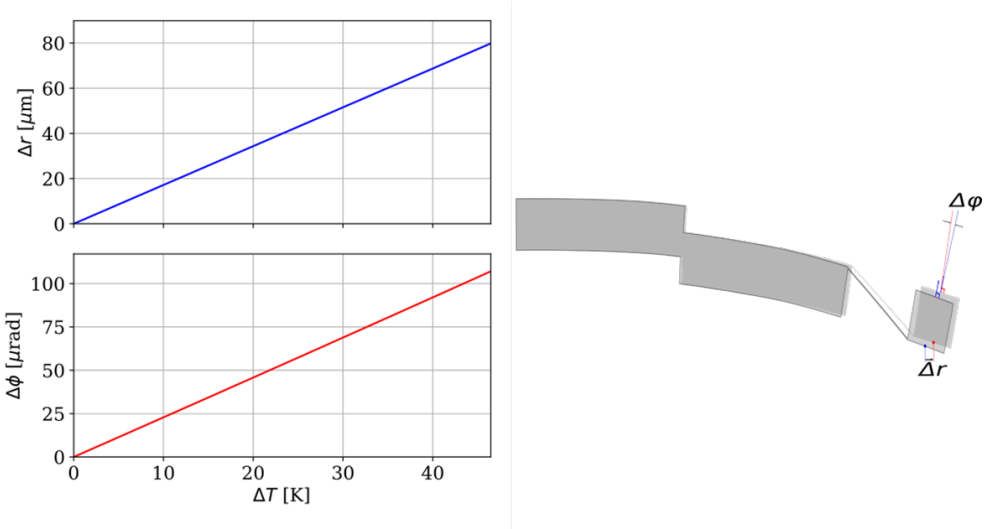

Figure 5: The rotation and radial expansion of the clearance holes in the outer ring of the T-SAMS actuator. The top left axes show the radial expansion of the location in the ring relative to the struts. The bottom left axes show the rotation of the central axis of the fastener.

Fig, 5 shows a rotation of the fastener axis of 100 µrad throughout the actuation range. This is expected to be negligible relative to the tolerance of the assembly.

In this simulation the maximum radial expansion of the fastener location is predicted to be 80 μm. As described in the previous section, for a rigid assembly this results in stress

significantly below the flexural strength of macor. For a strut length of 57mm the rotation across the full actuation range is 4.7 mrad. For a rigid assembly this results in the a fore mentioned torque of 0.5 Nm.

References

Corning SAS. MACOR®Machinable Glass Cermaic for Industrial Applications. 7 bis avenue de Valvins, CS 70156 Samois-sur-Seine, 77215 AVON Cedex, France.